9066 *Inorg. Chem.* **2009**, *48*, 9066–9068
DOI: 10.1021/ic901610j

Inorganic Chemistry
Communication

One-Dimensional Cyanide-Bridged $Mn^{III}W^{V}$ Bimetallic Complexes: Metamagnetism, Spontaneous Resolution, and Slow Magnetic Relaxation

Seok Woo Choi,[†] Dae Won Ryu,[†] Jin Wuk Lee,[†] Jung Hee Yoon,[†] Hyoung Chan Kim,[‡] Hyosug Lee,[§] Beong Ki Cho,[∥] and Chang Seop Hong*,[†]

[†]*Department of Chemistry (BK21), Korea University, Seoul 136-713, Korea,* [‡]*National Fusion Research Institute, Daejeon 305-333, Korea,* [§]*Hybrid Materials Group, Materials Research Laboratory, SAIT, Yongin City 446-712, Korea, and* [∥]*Department of Materials Science and Engineering Gwangju Institute of Science and Technology (GIST), Gwangju 500-712, Korea*

Received August 11, 2009

The reaction of $[W(CN)_6(bpy)]^-$ with the corresponding Mn Schiff bases led to the formation of two antiferromagnetic (**1**) and ferromagnetic (**2**) chains. The formation of the conglomerate (**2**) is associated with chiral induction by the enantiomeric chelate-ring conformation of the Mn Schiff base. Modulation of the linking groups in the Mn Schiff bases affects the interchain contacts, causing alteration of the magnetic behaviors from metamagnetism (**1**) to slow magnetic relaxation (**2**).

One of the remarkable advances in molecular magnets has involved the combination of magnetism with chirality since magnetochiral dichroism effects were discovered in paramagnetic and long-range-ordered materials.[1] Recently, a new class of magnetically anisotropic species, single-chain magnets, has become a current topical issue, and attempts to incorporate chiral characters were successfully carried out.[2]

The generation of chiral species can be achieved by using not only chiral components with stereogenic centers but also achiral substances via a spontaneous resolution process upon crystallization.[3,4] In fact, the latter provides a segregation of two types of enantiomorphic crystals, which is called a conglomerate. The phenomenon of conglomerate formation does not occur very often and is even hardly predictable because centrosymmetric crystals are preferably precipitated for thermodynamic and kinetic reasons.[5] Understanding whether a complex with an achiral ancillary affords a racemate or a conglomerate still remains elusive. However, collective efforts to fabricate chiral systems through spontaneous resolution and inductive explanations for the observations revealed that chiral crystals may be stabilized by directional intermolecular noncovalent forces (hydrogen bonds and/or $\pi-\pi$ contacts) and coordination bonds.[6] When a prediction of the crystal structure on the basis of the bonding interactions is more feasible, it is ultimately possible to control the crystal chirality at hand and applicable to broad academic and industrial areas.

To gain in-depth insight into conglomerate formation, factors in the structural components that ultimately affect the spontaneous resolution process are highly sought. We have attempted to employ quadridentate Schiff bases in which linking groups can be tuned to generate chiral centers. In this Communication, we present the syntheses, structures, and magnetic characterizations of a one-dimensional (1D) antiferromagnetic chain $[W(CN)_6(bpy)][Mn(L1)]\cdot MeCN\cdot 3H_2O$ (**1**$\cdot MeCN\cdot 3H_2O$; bpy = 2,2′-bipyridine, H_2L1 = *N*,*N*′-bis(2-hydroxynaphthalene-1-carbaldehydene)-1,2-diaminopropane] and a conglomerate of a 1D chiral ferromagnetic compound $[W(CN)_6(bpy)][Mn(L2)]\cdot MeCN\cdot H_2O$ (**2**$\cdot MeCN\cdot H_2O$; H_2L2 = *N*,*N*′-bis(2-hydroxynaphthalene-1-carbaldehydene)-1,2-diaminoethane]. The enantiomeric chelate-ring conformation of the $[Mn(L2)]^+$ entity is relevant

---

*To whom correspondence should be addressed. E-mail: cshong@korea.ac.kr.

(1) (a) Rikken, G. L. J. A.; Raupach, E. *Nature* **1997**, *390*, 493. (b) Inoue, K.; Kikuchi, K.; Ohba, M.; Okawa, H. *Angew. Chem., Int. Ed.* **2003**, *42*, 4810. (c) Coronado, E.; Galán-Mascarós, J. R.; Gómez-García, C. J.; Martínez-Agudo, J. M. *Inorg. Chem.* **2001**, *40*, 113.

(2) (a) Caneschi, A.; Gatteschi, D.; Lalioti, N.; Sangregorio, C.; Sessoli, R.; Venturi, G.; Vindigni, A.; Rettori, A.; Pini, M. G.; Novak, M. A. *Angew. Chem., Int. Ed.* **2001**, *40*, 1760. (b) Clérac, R.; Miyasaka, H.; Yamashita, M.; Coulon, C. *J. Am. Chem. Soc.* **2002**, *124*, 12837. (c) Yoon, J. H.; Ryu, D. W.; Kim, H. C.; Yoon, S. W.; Suh, B. J.; Hong, C. S. *Chem.—Eur. J.* **2009**, *15*, 3661. (d) Liu, T.-F.; Fu, D.; Gao, S.; Zhang, Y.-Z.; Sun, H.-L.; Su, G.; Liu, Y.-J. *J. Am. Chem. Soc.* **2003**, *125*, 13976. (e) Train, C.; Gheorghe, R.; Krstic, V.; Chamoreau, L.-M.; Ovanesyan, N. S.; Rikken, G. L. J. A.; Gruselle, M.; Verdaguer, M. *Nat. Mater.* **2008**, *7*, 729. (f) Bogani, L.; Vindigni, A.; Sessolia, R.; Gatteschi, D. *J. Mater. Chem.* **2008**, *18*, 4750.

(3) (a) You, Y. S.; Yoon, J. H.; Kim, H. C.; Hong, C. S. *Chem. Commun.* **2005**, 4116. (b) Inoue, K.; Imai, H.; Ghalsasi, P. S.; Kikuchi, K.; Ohba, M.; Okawa, H.; Yakhmi, J. V. *Angew. Chem., Int. Ed.* **2001**, *40*, 4242. (c) Coronado, E.; Gómez-García, C. J.; Nuez, A.; Romero, F. M.; Waerenborgh, J. C. *Chem. Mater.* **2006**, *18*, 2670. (d) Kaneko, W.; Kitagawa, S.; Ohba, M. *J. Am. Chem. Soc.* **2007**, *129*, 248.

(4) (a) Chen, X.-D.; Du, M.; Mak, T. C. W. *Chem. Commun.* **2005**, 4417. (b) Murphy, D. L.; Malachowski, M. R.; Campana, C. F.; Cohen, S. M. *Chem. Commun.* **2005**, 5506. (c) Gao, E.-Q.; Yue, Y.-F.; Bai, S.-Q.; He, Z.; Yan, C.-H. *J. Am. Chem. Soc.* **2004**, *126*, 1419.

(5) Pérez-García, L.; Amabilino, D. B. *Chem. Soc. Rev.* **2002**, *31*, 342.

(6) (a) Norsten, T. B.; McDonald, R.; Branda, N. R. *Chem. Commun.* **1999**, 719. (b) Lightfoot, M. P.; Mair, F. S.; Pritchard, R. G.; Warren, J. E. *Chem. Commun.* **1999**, 1945.

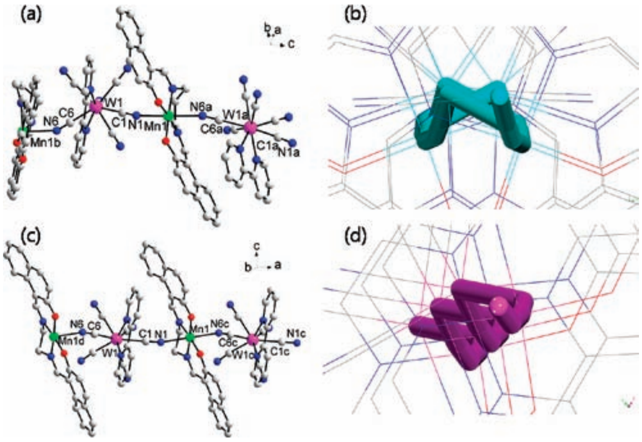

Figure 1. (a) Molecular view with a selected atom-labeling scheme and (b) diagram of a chain of **1** running down the *c* axis. (c) Molecular view with a selected atom-labeling scheme and (d) illustration of a left-handed (M) helical chain of **2**. Symmetry transformations used to generate equivalent atoms: $a = x, 1 - y, 0.5 + z$; $b = x, 1 - y, -0.5 + z$; $c = 1 + x, y, z$; $d = -1 + x, y, z$.

to chiral induction, finally generating spontaneous resolution of **2**. Modulation of noncovalent interchain forces renders the magnetic behaviors to vary from metamagnetism (**1**) to slow magnetic relaxation (**2**).

A stoichiometric reaction of $(PPh_4)[W(CN)_6(bpy)]$[7] with the respective Mn Schiff bases yielded deep-brown crystals of **1** and **2**. In the IR spectra, the characteristic CN stretching vibrations are found at 2162w, 2139w, 2125w, and 2118w cm^{-1} for **1** and at 2168w and 2131w cm^{-1} for **2**. The presence of bridging CN ligands is evidenced by peak shifts toward higher frequencies compared to the IR peaks of the precursor.

With the use of subtly different Schiff bases, complex **1** crystallizes in the monoclinic system with the space group *Cc*, while, interestingly, complex **2** belongs to the chiral orthorhombic space group $P2_12_12_1$. In the X-ray structures (Figure 1), each W ion, coordinated by six C atoms from CN groups and two N atoms from bpy, adopts a distorted square-antiprism (SAPR) geometry for **1** and an intermediate between a SAPR and a dodecahedron (DD) for **2** (Table S1 in the Supporting Information). The average bond lengths of W−C and W−N are 2.20(4) and 2.221(4) Å for **1** and 2.16(2) and 2.19(2) Å for **2**, respectively. The maximum deviation from 180° is 3.7° for **1** and 5.0° for **2**. In the Mn^{III} moieties, the Jahn−Teller distortion exists as judged from the elongated axial bond lengths [Mn1−N1 = 2.340(7) Å and Mn1−N6a = 2.315(7) Å for **1**, $a = x, 1 - y, 0.5 + z$; Mn1−N1 = 2.344(11) Å and Mn1−N6c = 2.349(9) Å for **2**, $c = 1 + x, y, z$] and the short equatorial Mn−N(O) lengths [mean Mn1−N(O) = 1.94(7) Å for **1** and 1.92(5) Å for **2**]. The magnetically important Mn−N−C(cyanide) angles are 165.0(6)° for Mn1−N1−C1, 152.3(6)° for Mn1−N6a−C6a (**1**), and 157.1(9)° for both Mn1−N1−C1 and Mn1d−N6−C6 (**2**). The average Mn−N−C angles are similar to each other.

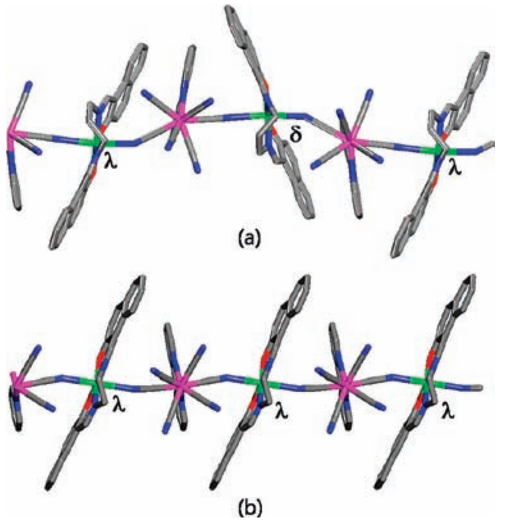

Figure 2. Enantiomeric chelate-ring conformations: (a) $-\lambda-\delta-\lambda-$ conformational sequence of chelate rings formed by propylenediamines of **1**; (b) $-\lambda-\lambda-\lambda-$ conformational sequence of chelate rings formed by ethylenediamines of **2**.

For **1**, the overall structure in the *ab* plane shows that chains are running along the *c* axis and are correlated with $\pi-\pi$-stacking forces between phenoxide rings and benzene rings of L1 (centroid distance = 3.569 Å) to form a three-dimensional array (Figure S1 in the Supporting Information). Hydrogen bonds among N atoms of unbound CN groups and lattice water O atoms (N2−O4 = 3.076 Å and O4−N3 = 2.871 Å) connect neighboring chains as well. The shortest interchain Mn−Mn distance is 10.626 Å. To assign the spatial conformations, we examined the backbones of chains. The Schiff bases in a chain of **1** have propylenediamine links that exhibit a $-\lambda-\delta-\lambda-$ conformational sequence of chelate rings, displaying no helicity in the chain. In contrast, the chelate rings formed by ethylenediamine linkages in **2** impart $-\lambda-\lambda-\lambda-$ discriminative conformations throughout the chain direction, resulting in a left-handed (M) helicity with a long pitch of 10.825 Å (Figure 2). Accordingly, the chirality is induced by the chiral center of the Mn(L2) Schiff base and propagated over the chain via the $[W(CN)_6(bpy)]^-$ subunits. This observation is compared with octacyanometalate-based racemates where $-\lambda-\lambda-\lambda-$ conformations of Mn(X−salen) (X = Cl, Br) give P helicity and $-\delta-\delta-\delta-$ sequences confer M helicity.[8] Thus, the molecular bridges are of importance because they seem to affect the overall helicity as observed. It appears that the chiral information is transferred into higher dimensionality via weak hydrogen bonds (Figure S2 in the Supporting Information). Phenoxide O atoms (O1) of chiral L2 ligands are interacted with lattice water molecules (O3), which act as additional H-atom donors to N atoms (N4) of free CN ligands (O1−O3 = 3.097 Å and O3−N4 = 3.018 Å). No $\pi-\pi$ contacts exist in **2**.

The thermal variation of the magnetic data of **1** is depicted in Figure 3a. The χ_mT value undergoes a gradual reduction upon cooling and reaches a minimum at 20 K. Below the valley temperature, χ_mT rises sharply. This feature is typical of the presence of intrachain antiferromagnetic interactions between W^V ($S_W = {}^1/_2$) and Mn^{III} ($S_{Mn} = 2$), which is also found in $[W(CN)_6(bpy)]^-$-based bimetallic complexes.[7a] Below 3 K, a downturn in χ_mT denotes the occurrence of interchain antiferromagnetic interactions. The fit of the

---

(7) (a) Choi, S. W.; Kwak, H. Y.; Yoon, J. H.; Kim, H. C.; Koh, E. K.; Hong, C. S. *Inorg. Chem.* **2008**, *47*, 10214. (b) Szklarzewicz, J. *Inorg. Chim. Acta* **1993**, *205*, 85.

(8) Yoo, H. S.; Ko, H. H.; Ryu, D. W.; Lee, J. W.; Yoon, J. H.; Lee, W. R.; Kim, H. C.; Koh, E. K.; Hong, C. S. *Inorg. Chem.* **2009**, *48*, 5617.

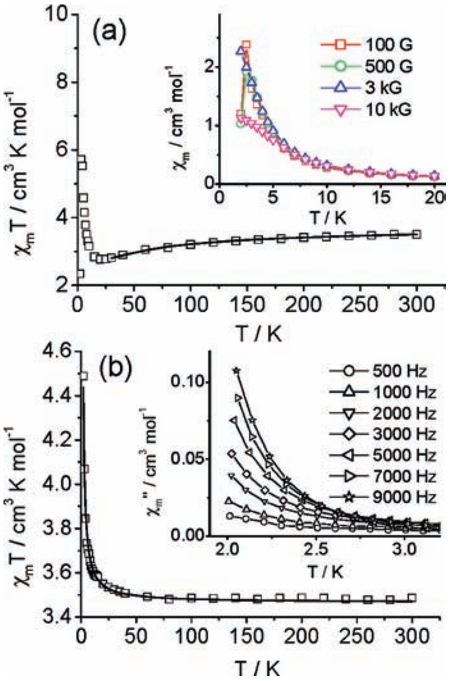

Figure 3. (a) Plot of $\chi_m T$ versus T for **1**. The inset shows plots of χ_m versus T at various fields. (b) Plot of $\chi_m T$ versus T for **2**. The inset indicates the temperature dependence of χ_m'' at several frequencies.

Drillon expression to the data at $T > 30$ K affords roughly estimated results of $g_{Mn} = 2.05$, $g_W = 2$, and $J = -9.4$ cm^{-1}.[9] The intrachain magnetic coupling constant J is similar to those of the analogous systems.[7a] A sigmoidal curve in the $M(H)$ plot (Figure S3 in the Supporting Information) indicates a field-induced metamagnetic transition from the interchain antiferromagnetic state to a ferrimagnetic phase with a saturation magnetization of 2.84 $N\beta$, which is close to 3 $N\beta$ calculated from $M_S = 2(S_{Mn} - S_W)$.[7a] The critical field (H_C) of 1800 G is determined by the derivative of M against H. The phase transition is ascertained by the χ_m plots (inset of Figure 3a), in which the weak interchain antiferromagnetic interactions mediated via the interchain contacts (hydrogen bonds and $\pi-\pi$ stackings) are overcome by an increase in the external magnetic field above H_C. The χ_m' and χ_m'' data were taken at a direct-current field of zero and an alternating-current field of 5 G, disclosing the frequency independence at a peak temperature of 2.6 K (Figure S4 in the Supporting Information). This is indicative of the onset of a long-ranged magnetic order probably arising from spin canting, which is associated with single-ion anisotropy and the lack of symmetry operations between adjacent Mn^{III} ions.[10]

The cryomagnetic data for **2** is noticeably different from those for **1** (Figure 3b). As the temperature is lowered, $\chi_m T$ increases steadily and then abruptly. This implies the clear existence of ferromagnetic interactions between W^V and Mn^{III}, which is in sharp contrast to **1** but consistent with the W^V−Mn^{III} tetramer.[11] The approximate fit gives $g_{Mn} = 2.03$, $g_W = 2$, and $J = 0.34$ cm^{-1}. The intrachain ferromagnetic coupling is also supported by the $M(H)$ curve at 2 K (Figure S5 in the Supporting Information). In the low-field regime, the Brillouin curve with $S = {}^5/_2$ agrees well with the experimental data, and a saturation magnetization of 4.11 $N\beta$ approaches the ferromagnetic arrangement (5 $N\beta$). The out-of-phase component (χ_m'') is frequency-dependent, which is a probable signature of the slow relaxation of the magnetization, and the lack of significant interchain contacts may be responsible for such behavior. Further analysis is hampered because maxima in χ_m'' were not observed down to 2 K.

To assess the magnetic couplings underlying these systems, we carried out density functional theory calculations on $[W(CN)_6(bpy)]^-$ moieties (Figure S6 in the Supporting Information). The spin density on the N end of bridging CN ligands is sizable in **1** but almost invisible in **2**. As a consequence, the magnetic exchange coupling via the π pathway of W−C≡N−Mn in **1** is effective enough to give the antiferromagnetic result, whereas the orbital overlap through the π route in **2** becomes minimal and eventually confers the ferromagnetic interaction.[12] This demonstrates that the central geometry around W (SAPR in **1** and SAPR/DD in **2**) plays a pivotal role in the magnetic coupling nature in these systems.[13]

In summary, two 1D chains constructed by $[W(CN)_6(bpy)]^-$ and anisotropic Mn Schiff bases have been prepared. Spontaneous resolution is associated with chiral induction by the enantiomeric chelate-ring conformations of $[Mn(L2)]^+$ in **2**. A degree of interchain contacts accounts for metamagnetism in **1** and slow magnetic relaxation in **2**.

Acknowledgment. This work was supported by Korea Science and Engineering Foundation (KOSEF) grants funded by the Korea government (MEST) (Grants 2009-0053164 and 2009-0071129). The work at GIST was supported by the WCU program at GIST through a grant provided by the Ministry of Education, Science and Technology (MEST) of Korea (Project No. R31-2008-000-10026-0).

Supporting Information Available: X-ray crystallographic files in CIF format and additional synthetic, structural, and magnetic data for **1** and **2**. This material is available free of charge via the Internet at http://pubs.acs.org.

---

(9) Drillon, M.; Coronado, E.; Beltran, D.; Georges, R. *Chem. Phys.* **1983**, *79*, 449.

(10) Hernández, M.; Lloret, F.; Ruiz-Pérez, C.; Julve, M. *Inorg. Chem.* **1998**, *37*, 4131.

(11) Yoon, J. H.; Lim, J. H.; Kim, H. C.; Hong, C. S. *Inorg. Chem.* **2006**, *45*, 9613.

(12) Kahn, O. *Molecular Magnetism*; VCH Publishers, Inc.: New York, 1993.

(13) Visinescu, D.; Desplanches, C.; Imaz, I.; Bahers, V.; Pradhan, R.; Villamena, F. A.; Guionneau, P.; Sutter, J.-P. *J. Am. Chem. Soc.* **2006**, *128*, 10202.